Ecological Modelling 221 (2010) 2793–2800

Contents lists available at ScienceDirect

Ecological Modelling

journal homepage: www.elsevier.com/locate/ecolmodel

Spatially mixed crops to control the stratified dispersal of airborne fungal diseases

Natalia Sapoukhina[a,b,c,*], Yuri Tyutyunov[c,d], Ivan Sache[e], Roger Arditi[f]

[a] INRA, UMR INRA/AGROCAMPUS OUEST/UA Plant Pathology, BP 60057, F-49071 Beaucouzé, France
[b] INRA, USC Écologie des populations et communautés, AgroParisTech, 16 rue Claude Bernard, 75231 Paris cedex 05, France
[c] Southern Federal University, Vorovich Research Institute of Mechanics and Applied Mathematics, Department of Mathematical Methods in Economics and Ecology, Laboratory of Mathematical Modelling of Biological Processes, Stachki str. 200/1, 344090 Rostov-on-Don, Russia
[d] Southern Scientific Center of Russian Academy of Sciences (SSC RAS), Chekhov str. 41, 344006 Rostov-on-Don, Russia
[e] INRA, UMR Bioger-CPP, AgroParisTech Campus, BP 01, 78850 Thiverval-Grignon, France
[f] INRA, USC Écologie des populations et communautés and CNRS, UMR Écologie et Évolution, Université Pierre et Marie Curie, Sorbonne Universités, 7 quai Saint-Bernard, case 237, 75252 Paris cedex 05, France

ARTICLE INFO

Article history:
Received 7 April 2010
Received in revised form 13 August 2010
Accepted 18 August 2010
Available online 15 September 2010

Keywords:
Fungal disease epidemiology
Diffusion model
Invasion
Long-distance dispersal
Resistance management

ABSTRACT

Intraspecific crop diversification is thought to be a possible solution to the disease susceptibility of monocultured crops. We modelled the stratified dispersal of an airborne pathogen population in order to identify the spatial patterns of cultivar mixtures that could slow epidemic spread driven by dual dispersal mechanisms acting over both short and long distances. We developed a model to simulate the propagation of a fungal disease in a 2D field, including a reaction-diffusion model for short-distance disease dispersal, and a stochastic model for long-distance dispersal. The model was fitted to data for the spatio-temporal spread of faba bean rust (caused by *Uromyces viciae-fabae*) through a discontinuous field. The model was used to compare the effectiveness of eight different planting patterns of cultivar mixtures against a disease spread by short-distance and stratified dispersal. Our combined modelling approach provides a reasonably good fit with the observed data for the spread of faba bean rust. Similar predictive power could be expected for the management of resource-mediated invasions by other airborne fungi. If a disease spreads by short-distance dispersal, random mixtures can be used to slow the epidemic spread, since their spatial irregularity creates a natural barrier to the progression of a smooth epidemic wave. In the context of stratified dispersal, heterogeneous patterns should be used that include a minimum distance between susceptible units, which decreases the probability of infection by long-distance spore dispersal. We provide a simple framework for modelling the stratified dispersal of disease in a diversified crop. The model suggests that the spatial arrangement of components in cultivar mixtures has to accord with the dispersal characteristics of the pathogen in order to increase the efficiency of diversification strategies in agro-ecosystems and forestry. It can be applied in low input agriculture to manage pathogen invasion by intercropping and cultivar mixtures, and to design sustainable systems of land use.

1. Introduction

Protecting crops against fungal diseases currently relies mainly on the use of fungicides and resistant varieties. There is an increasing demand for a drastic reduction in the use of fungicides (Aubertot et al., 2005), which are expensive, unfriendly towards the environment and people, and are increasingly becoming less effective against pathogens. Similarly, the incautious planting of monocultures of resistant varieties on large acreages has led to the selection of virulent pathogens that are able to overcome plant resistance; there are many examples of resistance breakdown of this type in a wide range of crops (Bayles et al., 2000; Rouxel et al., 2003; Guérin and Le Cam, 2004; Van Den Bosch and Gilligan, 2003), the most recent important event of this kind being the appearance and spread of strain *Ug99* of wheat stem rust, which threatens wheat production in Asia and, possibly, worldwide (Singh et al., 2006; Jin et al., 2008).

Re-diversification of crops to limit the yield losses caused by pathogens and to increase the durability of varietal resistance has been advocated for decades, as reviewed by Finckh and Wolfe (2006). Theoretical and experimental studies have demonstrated the effectiveness of intercropping (Bouws and Finckh, 2008), and

* Corresponding author at: INRA, UMR INRA/AGROCAMPUS OUEST/UA Plant Pathology, BP 60057, F-49071 Beaucouzé, France. Tel.: +33 2 41 22 57 17; fax: +33 2 41 22 57 05.
E-mail address: Natalia.Sapoukhina@angers.inra.fr (N. Sapoukhina).

0304-3800/$ – see front matter © 2010 Elsevier B.V. All rights reserved.
doi:10.1016/j.ecolmodel.2010.08.020

of using mixtures of susceptible and resistant varieties in disease management (Xu and Ridout, 2000; Mundt, 2002; Skelsey et al., 2005). It has been shown that cultivar mixtures can be more profitable than pure stands of the constituent cultivars (Manthey and Fehrmann, 1993). Varietal mixtures limit the spread of disease by lowering the density of susceptible plants, thus increasing the distance between them; the effectiveness of mixtures in terms of disease control is therefore determined to a considerable extent by the spatial arrangement of the components of the mixture (Xu and Ridout, 2000; Didelot et al., 2007; Sapoukhina et al., 2009). However, most experimental studies and simulation models have only considered the short-distance dispersal of the pathogen within a plot, whereas airborne fungi can also spread discontinuously over very large distances. The relevant spatial scale for evaluating varietal mixtures should consist of at least an array of plots. However, it is quite difficult to carry out experiments in such a field system (however, see Zhu et al., 2000; Soubeyrand et al., 2007), and so preliminary simulations are called for in order to address the main questions raised by the deployment of varietal mixtures before carrying out field trials.

A first step towards understanding the effect of varietal mixtures on disease epidemics is to investigate the spatial properties of the mechanisms governing pathogen population dispersal, in order to highlight the factors that can either accelerate the spread of disease or slow it down. Recent studies of biological invasions have shown that the expansion of a species is driven by two main modes of dispersal: neighborhood diffusion, in which individuals immigrate to areas adjacent to the parent colony, resulting in a focal dispersal; and long-distance dispersal, when offspring colonies develop at some distance from the parent colony due to stochastic, long-distance jumping by individuals. These two modes of dispersal very often occur side-by-side within a species, thus stratifying the dispersal process. Hengeveld (1989) coined the term of "stratified diffusion" to describe the pattern that emerged from field observations and theoretical studies of the combination of short- and long-distance dispersal processes in biological invasions.

Invasion processes have usually been modelled using adapted diffusion and reaction-diffusion models (Andow et al., 1990; Murray, 1993; Hengeveld, 1994; Shigesada and Kawasaki, 1997; Okubo and Levin, 2002). Although diffusion models are good descriptors of the massive invasion of a homogeneous landscape, resulting from short-range, random movements (Skellam, 1951), they are less suitable for describing less frequent movements over longer distances. One of the main shortcomings of diffusion models is that they assume the continuous spread of a disease focus expanding at constant rate. Only a few of the many methods that have been proposed for modelling long-distance dispersal (reviewed by Nathan et al., 2003) are really appropriate for studying stratified dispersal (Shigesada et al., 1995; Sharov and Liebhold, 1998; Higgins and Richardson, 1999). Existing phenomenological models of stratified dispersal cannot be applied to crop protection, since they do not explicitly consider the spatial characteristics of the landscapes invaded. In particular, we know little about the consequences of the spatial patterning of plant varieties for the management of disease with diffusive and stratified dispersal.

The goal of the present study was to identify the spatial patterns of cultivar mixtures that can be used to slow epidemic spread driven by dual dispersal mechanisms acting over both short and long distances. This enables us to ask whether these spatial arrangements of varieties can be used to control plant diseases characterised by a short-distance and stratified dispersal, or whether spatial diversification strategy has to be tailored to the dispersal mode of the disease.

First, we designed a model of the spread of an airborne fungal disease that explicitly included a dual (i.e., short- and long-distance) dispersal process. The simulation model consisted of a reaction-diffusion submodel of the dynamics of susceptibles, infectives and spores, which produces continuous, local disease spread, coupled with a stochastic algorithm that mimics long-distance spore dispersal. We also explicitly modelled the dual dispersal process focusing on the spatial factors that affect the rate of disease spread. We checked and validated the model's predictions versus a case study providing extensive field data on the spread of a typical airborne fungal disease, faba bean rust (caused by *Uromyces viciae-fabae*) over a heterogeneous field (Sache and Zadoks, 1996). Second, we used the parameter values obtained to perform numerical simulations to assess the effect of patterning varietal mixtures on the spread of disease by stratified dispersal. Finally, we discuss the role of spatial structuring in crop diversification strategies.

2. Materials and methods

2.1. Model of short-distance dispersal

In this section we present a model of the focal expansion of a fungal disease propagated by airborne spores in a two-dimensional environment $D = [0, L_x] \times [0, L_y]$ (m^2). The spatial scale of the environment, D, depends on the pattern of disease dispersal being studied. We assume that continuous disease propagation results from the contact between susceptible leaf tissue $S(\mathbf{x},t)$ (leaf area, m^2, per surface, m^2) and deposited spores $P(\mathbf{x},t)$ (mg m^{-2}), followed by the appearance of infected tissue, i.e., lesions, $I(\mathbf{x},t)$ (lesions m^{-2}). These lesions then produce spores that are dispersed randomly to localities in the immediate neighborhood. We consider the dynamics of interacting populations during a cropping season, from spring till harvest, and time t is measured in days (d). Assuming that the rate of epidemic spread is much higher than the rate of crop growth (Soubeyrand et al., 2007), our model ignores the latter. We use a reaction-diffusion model to describe the focal pattern of disease development and its spatial spread:

$$\begin{aligned} \frac{\partial S}{\partial t} &= -aPS, \\ \frac{\partial I}{\partial t} &= ePS - mI, \\ \frac{\partial P}{\partial t} &= \varepsilon I - \mu P + \delta\ \Delta P, \end{aligned} \tag{1}$$

where the contact coefficient, a, represents the area that can be covered by a unit of spore biomass in a unit of time. Parameter e is a measure of the efficiency of disease transmission from infected leaf tissue to susceptible plants. Parameter ε is the spore density produced by a unit of infected biomass per unit of time. Infected tissue has a mortality rate of m. We assume that at each moment of time μP spores escape local deposition. The rate of focal spread is represented by the diffusion coefficient, δ. The definitions and units of the parameters are presented in Table 1. We assume that the system in Eq. (1) is an open system, i.e., it has a passive boundary.

2.2. Stochastic algorithm for long-distance dispersal

Model Eq. (1), describing epidemic propagation from an inoculum source to neighboring localities, is coupled with a stochastic algorithm simulating long-distance spore dispersal. Before describing the algorithm, let us consider how diffusive model Eq. (1) works. To solve the PDE system, we approximated it to an ODE system using a finite differences method. As a result, the two-dimensional field, D, becomes a grid consisting of $n \times k$ units $\Delta x \times \Delta y$ in size, where $\Delta x = L_x/n$ and $\Delta y = L_y/k$. The ODE system obtained, consisting of $n \times k$ equations with an initial condition (S_0, I_0, P_0), is then integrated numerically by the fourth-order Runge–Kutta method with an adaptive time step, Δt (Press et al., 1992). At each time step Δt (d) at each grid point $(i\Delta x, j\Delta y)$, $i = 1 \ldots n$, $j = 1 \ldots k$, we get a system

Table 1
Definition and values of the parameters used to model faba bean rust dynamics, and results of the sensitivity analysis. Estimated values are reported with standard errors between brackets. The elasticity, E, of predicted disease severity to model parameters. Parameters varied ± 5%.

Parameter	Definition (units)	Measured value	Estimated value	Elasticity, E
$S_0(\mathbf{x}, 0)$	Initial density of susceptible leaf area	1		±2.83
$I_0(\mathbf{x}, 0)$	Initial lesion density (lesions m^{-2})	0		
Δx	Sideways distance between two field points (m)	0.3		
Δy	Lengthways distance between two field points (m)	0.3		
L_x	Field width (m)	51.9		
L_y	Field length (m)	79.8		
a	Contact rate (m^2 mg^{-1} d^{-1})	0.17		±0.3
ε	Spore production rate (mg $lesion^{-1}$ d^{-1})	0.011		±2.77
e	Infection efficiency (lesions mg^{-1} d^{-1})	3.74		±2.86
δ	Diffusion coefficient (m^2 d^{-1})	0.07		±0.13
m	Mortality rate of infectives (d^{-1})		8.4E−10 (4.0E−12)	±0.05
μ	Spore removal rate (d^{-1})		1.74E−6 (5.9E−8)	±2.14
$P_0(\mathbf{x}, 0)$	Spore density of the initial inoculum (mg m^{-2})		0.04 (0.9E−3)	±0.27
λ	Long-distance dispersal rate (d^{-1})		0.24 (3.3E−3)	±0.06

solution, and hence the densities of susceptibles $S(\mathbf{x},t)$, infectives $I(\mathbf{x},t)$ and spores $P(\mathbf{x},t)$ over the two-dimensional field D, $\mathbf{x}\in D$. This results in dynamic redistribution of the population densities in a 2D area from an initial local inoculum of P_0 (mg m^{-2}) spores. If we inoculate several space units we will observe foci regularly expanding from each of them. This means that we can simulate infrequent LDD events by incorporating an algorithm governing spore deposition into random space units, X and Y, into the process of numerical solution. We assume the emergence of the secondary foci to be a branching process: at each time step, Δt, any focus, i, can produce $\varphi_i(\Delta t)$ secondary foci and $\sum_i \varphi_i = \Phi(\Delta t), \Phi \in N$. The number of foci produced in Δt increases exponentially with time, and is limited only by the availability of susceptible hosts and spores. Thus, the distribution of random spatial coordinates of the secondary foci X and Y can be approximated by a uniform distribution law. Indeed, at a certain level of the density of foci in space, D, the probability that any given spatial point $(i\Delta x, j\Delta y)$ will be infected becomes almost identical. To model the spread of disease by long-distance dispersal, we repeat steps 1–4 at each time step, Δt:

1. Calculation of the quantity of spores available for long-distance dispersal. This quantity (mg d^{-1}), is assumed to be proportional to the total spore biomass over the field, $\lambda \int_D P(\mathbf{x}, t)d\mathbf{x}$. Here, λ (d^{-1}) is the rate of long-distance dispersal.
2. We assume that inoculating with P_0 spores (mg m^{-2}) is enough to infect a susceptible unit measuring $\Delta x \times \Delta y$, and lead to subsequent epidemic spread to neighboring localities. Thus, by dividing $\lambda \int_D P(\mathbf{x}, t)d\mathbf{x}$ (mg d^{-1}) by $P_0\,\Delta x\,\Delta y$ (mg) we can estimate how many units can potentially be infected. This gives us the deposition rate $\Phi(t) = \left[(\lambda/(P_0\,\Delta x\,\Delta y))\int_D P(\boldsymbol{x}, t)\,d\boldsymbol{x}\right]$ (d^{-1}) that regulates the frequency of spore deposition by LDD (here, square brackets [...] mean rounded to the next integer).
3. We derive $\Phi(t)$ random coordinates $i\Delta x$ and $i\Delta y$, $i = 1 \ldots \Phi(t)$, from the uniform distribution law in the intervals $(0, n)$ and $(0, k)$, respectively.
4. In each unit of this random sample, P_0 spores are deposited and model Eq. (1) initiates disease growth and its spread to neighboring units. If a given spatial unit does not contain any susceptible host tissue, the spores deposited there are lost. For a recurring spatial unit in the random sample, the epidemic focus is produced from a high concentration inoculum.

To summarize, long-distance dispersal is driven by two parameters: the rate λ (d^{-1}), which determines the spore biomass available for long-distance dispersal, and the spore density for a primary inoculum, P_0 (mg m^{-2}). This latter parameter is derived from diffusion model Eq. (1), and so only λ has to be estimated for the LDD algorithm. The resulting model was implemented in Borland Delphi V4.5. The code is available upon request.

2.3. Case study: the spread of faba bean rust

The spatio-temporal spread of an epidemic of faba bean rust was monitored over a heterogeneous field, and has been described elsewhere (Sache and Zadoks, 1996). We therefore omit some aspects, and concentrate on the factors that were used to test our modelling approach.

In a maize field (D = 80 m × 50 m), plots were sown with a faba bean variety that is highly susceptible to rust. The 'source plot' consisted of 13 × 13 units (each unit containing 2–7 stems produced from 3 seeds), planted at a center-to-center distance of 0.3 m. Thirty-three 'trap plots' were established following a regular pattern (Fig. 1). Five rows of trap plots were established 10 m, 20 m, 30 m, 35 m and 40 m downwind of the source plot, respectively. Three trap plots were established 10-m upwind from the source plot. The distance between plots within rows was 10 m. Each trap plot consisted of 3 × 3 units, planted at a center-to-center distance of 0.3 m. The central unit of the source plot was inoculated 69 days after planting. The experiment was devised in such a way that this inoculum was the only source of disease. Disease severity was assessed up to 59 days after inoculation. The sporulating lesions were counted on each leaf, and 40 sporulating lesions per leaf were considered to be equal to 1% severity. The mean severity was evaluated for each unit by averaging the severity values recorded for all the leaves in the unit.

Examining epidemic spread over a whole field, Sache and Zadoks (1996) concluded that the observed pattern of disease progression was explained by a dual dispersal mechanism: short-distance dispersal within the source plot, and a long-distance, stochastic, plot-to-plot dispersal over the entire discontinuous field. We reanalyzed these field data to highlight the main characteristics of short-distance dispersal and long-distance dispersal, and to parameterize the model.

2.4. Parameter estimation

We parameterized the model using epidemiological data for faba bean rust (*Uromyces viciae-fabae*). Most of these parameter values were derived from the results of controlled-condition experiments performed with faba bean rust (Sache and Zadoks, 1995).

2.4.1. Contact rate (a)

The inoculation of 1 mg of spores resulted in a deposited spore density of 100 spores cm^{-2} or 10^6 spores m^{-2} (Sache and Zadoks, 1995). Since 1 mg of freshly collected spores yields about 170,000

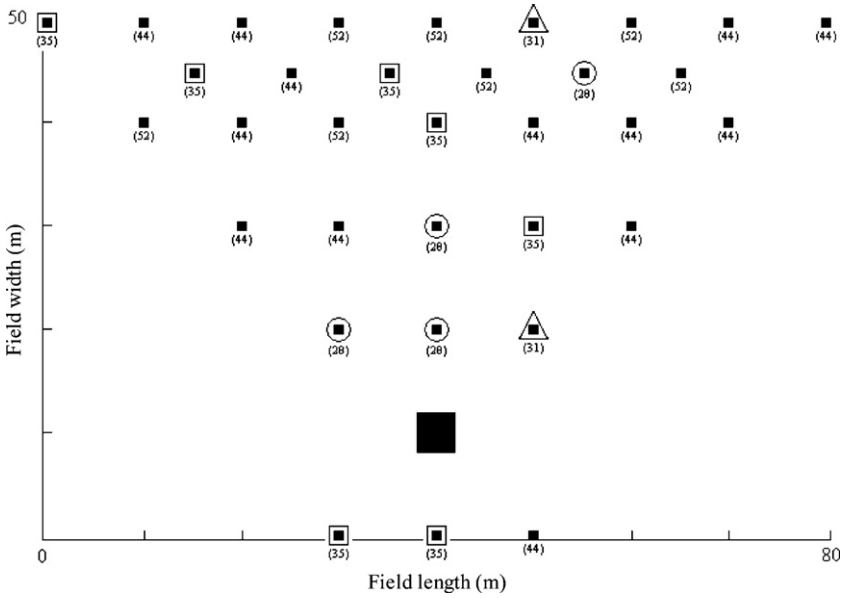

Fig. 1. Layout of the experiment used as a case study. The big square represents the source plot; the smaller squares represent the trap plots. Distances are given in m, and plot representation is not scaled. The entries below the plots indicate the times when rust was first detected in the plot (28 days: plots in a circle; 31 days: plots in a triangle; 35 days: plots in a square).

uredospores (Sache and Zadoks, 1995), the deposited spore density transforms to $10^2/17\,\mathrm{mg\,m^{-2}}$. It results in a contact rate of $a = 0.17\,\mathrm{m^2\,mg^{-1}\,day^{-1}}$.

2.4.2. Rate of spore production (ε)

The total spore production per lesion was about $(9.3 \pm 2.5) \times 10^4$ spores lesion^{-1}, obtained over a period of 50 days following a latency period of 8–10 days (Sache and Zadoks, 1995). A spore production of 9.3×10^4 spores lesion^{-1} over 50 days gives a rate of $\varepsilon = 1860$ spore lesion^{-1} d^{-1} or, in milligrams, $\varepsilon = 0.011$ mg lesion^{-1} d^{-1}.

2.4.3. Infection efficiency (e)

In empirical studies, the infection efficiency is measured as the ratio of the number of sporulating lesions per cm^{-2} to the number of spores deposited per cm^{-2}. For faba bean rust, infection efficiency was evaluated as 0.11 lesion per 100 deposited spores per cm^{-2} (Sache and Zadoks, 1995). Converting to mg of spores and for a period of 50 days, we obtain $e = 0.0011 \times 17 \times 10^4/50 = 3.74$ lesions mg^{-1} d^{-1}.

2.4.4. Diffusion coefficient (δ)

We estimate the diffusion coefficient using $\delta = M_S(t)/4t$, where $M_S(t)$ is the mean square displacement of organisms, and t is the number of time units since their release (Andow et al., 1990). Knowing that within 11 days the disease had spread from the central infected unit to the boundary of the source plot, an area of 3.24 m^2 (Sache and Zadoks, 1996), we obtain $\delta = 0.07\,\mathrm{m^2\,d^{-1}}$.

2.4.5. Model fitting

We therefore fixed the values of four significant parameters, a, ε, e, δ (Table 1) and assessed the values of mortalities, m, μ, of the density of initial spore deposition, P_0, and the LDD rate, λ, by fitting. We fitted model Eq. (1) with $M = 3$ adjustable parameters $\boldsymbol{\rho} = (m, \mu, P_0)$ to N_1 observations of the mean disease severity of the homogeneous source plot, (t_i, y_i), $i = 1, \ldots, N_1$ (Fig. 2a), and a parameter of LDD algorithm, $\boldsymbol{\rho} = \lambda$, $M = 1$, to N_2 observations of the mean severity in 33 trap plots (Fig. 2b). Data measurement errors are assumed to be independent and normally distributed with constant standard deviation. At a given time, t_i, the model disease severity is calculated as the percentage of the total number of lesions over the plot to the total initial density of susceptibles, $y(t_i, \boldsymbol{\rho}) = 100\,\%\,(a/e/S_0) \int_D I(\mathbf{x}, t_i) d\mathbf{x}$. The maximum likelihood estimate of the model parameters is obtained by minimizing the merit function as follows: $F(\boldsymbol{\rho}) = \sum_{i=1}^{N} (y_i - y(t_i, \boldsymbol{\rho}))^2$, $N \in \{N_1, N_2\}$, defined as the sum of squared residuals between the experimental data, and the corresponding model output. The parameters of the model are then adjusted to minimize the merit function, yielding the best-fit parameters. To minimize the merit function over M parameters, we used the simplex-simulated annealing approach (SSA) for the global optimization, which combines the downhill simplex and simulated annealing algorithms (Press et al., 1992). To assess the accuracy of the evaluated values of the parameters we used residual bootstrapping (Efron and Tibshirani, 1993). To assess the fit of the SDD model and the LDD algorithm we calculated the coefficient of determination as $R^2 = \sum_{i=1}^{N} (y(t_i, \boldsymbol{\rho}) - \bar{y})^2 / \sum_{i=1}^{N} (y_i - \bar{y})^2$, where

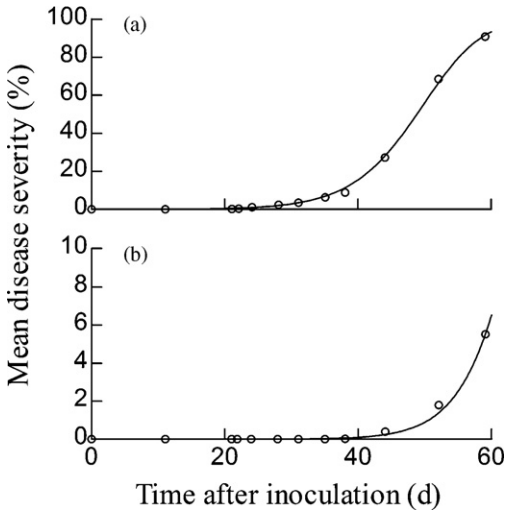

Fig. 2. Observed (circles) and predicted (curves) spread of faba bean rust under field conditions (Fig. 1). (a) Temporal dynamics of mean disease severity in the source plot. (b) Temporal dynamics of mean disease severity in 33 trap plots. Parameter values are presented in Table 1.

$\bar{y}$ denotes the mean of the observations and $N \in \{N_1, N_2\}$. R^2 estimates the proportion of the observed variability that is explained by the model. The higher the R^2 value, the better the fit of the model, with $R^2 = 1$ denoting a perfect fit.

2.4.6. Sensitivity analysis

The purpose of the analysis was to test how model predictions respond to perturbations of the model parameters, and thus to identify the most critical parameters. Since a global sensitivity analysis was beyond the scope of our study, we confined the sensitivity analysis to the case of a discontinuous field (Fig. 1). The area under the disease progress curve (AUDPC) (Shaner and Finney, 1977) calculated over a 60-day period following inoculation was chosen as a state variable for the analysis. AUDPC is a summary variable of disease progress: a high AUDPC is indicative of rapid disease progress. Simulations for the fitted parameter values (Table 1) serve as the baseline model. A variety of parameters: epidemiological parameters (contact rate, rate of spore production, infection efficiency, mortality rate of infectives, removal rate of spores), dispersal parameters (diffusion coefficient, long-distance dispersal rate) and the initial state (density of the pathogen spore inoculum, susceptible leaf area), varied by ±5% of their values in the baseline model. The proportional sensitivity (elasticity), E, of the state variable, AUDPC, was calculated as

$$E = \frac{\rho_b}{\mathrm{AUDPC}_b} \frac{\partial \mathrm{AUDPC}}{\partial \rho}, \quad (2)$$

where ρ_b and AUDPC_b are the values from the baseline simulation, and $\partial \mathrm{AUDPC}/\partial \rho$ is linearly approximated using the results from the perturbation runs. The elasticity quantifies the relative contribution of ρ to the area under the disease progress curve.

2.5. Numerical simulations

We performed numerical simulations using estimated parameter values to assess different spatial patterns of a crop as a means of controlling disease propagation driven by stratified dispersal. We designed a simulation field of 51.9 m × 79.8 m corresponding to the real field presented in Fig. 1. According to the applied numerical method for solving system Eq. (1), the field contains 46 458 discrete cells of $\Delta x \times \Delta y = 0.3$ m × 0.3 m size. We represented different crop patterns by filling the cells with 1 or 0, where 1 corresponds to the susceptible host, and 0 to the resistant host.

Since random distribution and alternating rows are the most popular patterns in diversification strategies (Mundt, 2002), we tested the following patterns: random mixture, narrow and frequent rows, wide and distant rows (Table 2). We also considered remote blocks (Table 2) as an alternative pattern to random irregularity and to row continuity. Such remote blocks can arise when distinct fields are distributed at the landscape scale. To examine the effect of the level of irregularity of the pattern on its efficiency, we designed 1:1 and 1:3 mixtures for each pattern. In 1:3 mixtures, the resistant surface was extended to three-quarters of the total host area. To create 1:3 regular patterns, {pt′2, pt′3, pt′4}, we kept the metrics of susceptible rows/blocks with the corresponding 1:1 patterns and increased the distance between them. Inoculating a randomly selected susceptible cell with $P_0 \times \Delta x \times \Delta y$ spores (mg), we simulated the onset of an epidemic from an external source. We compared the efficiency of the patterns by estimating the mean time for disease severity to reach 80%, $T_{\mathrm{pt}}^{80\%}$, and a relative spread deceleration of disease $D_{\mathrm{pt}}(\%) = \left(T_{\mathrm{pt}}^{80\%}/T_{\mathrm{pt0}}^{80\%} - 1\right) \times 100$, pt∈ {pt1, pt′1, . . ., pt4, pt′4}, measuring the impact of the geometry of spatial arrangement of susceptible and resistant varieties on the pathogen spread rate compared to the purely homogenous susceptible pattern, pt0. In the case of stratified dispersal, for each pattern, pt∈ {pt1, pt′1, . . ., pt4, pt′4}, we performed Monte Carlo simulations running 1000 replications of the model in order to estimate the mean spread deceleration D_{pt} and its confidence interval.

3. Results

3.1. Invasion reconstruction

To analyze the pattern of epidemic propagation through the field, we considered the dynamics of disease severity. We assessed $N_1 = 11$ and $N_2 = 7$ nonzero data points for the mean disease severity in the source (Fig. 2a) and trap (Fig. 2b) plots, respectively. Analysis of time-series data showed that in the source plot measuring 15.21 m^2, disease spread mainly followed a focal pattern; there were no major foci located far from the epidemic front. The disease developed extremely fast, so that all units had been infected by day 31. The radial velocity of expansion was calculated as $c = 0.09$ m d^{-1} (Sache and Zadoks, 1996). The data points obtained (Fig. 2a and b), coupled with the estimation of the spread velocity, were used to calibrate model Eq. (1), which describes short-distance dispersal.

Analysis of the epidemic propagation in the trap plots showed that the first rust lesions were detected on day 28 in four plots located in the rows nearest to the source plot (10–20 m from it), while another lesion was detected in the fourth row, 35 m away (Fig. 1). At this time, the mean disease severity in the source plot was 2.5%, that is 0.11 lesions cm^{-2}. This means that even a low disease density was able to produce enough spores for long-distance dispersal to occur. A week later, on day 35, another seven infected units were detected in different plots. The most distant infected plot was located in the last row, 57 m from the center, quite some distance from the other infected plots. The observation on day 44 showed that only seven plots remained uninfected, and these were located in the last three rows. All plots had been infected by day 52. Fig. 2b summarizes disease progress in all the trap plots, which were further used to parameterize the long-distance dispersal algorithm.

3.2. Model fitting

Smooth lines in Fig. 2 depict the fit between model Eq. (1) and the experimental data of rust spread over the source plot and trap plots. The data quite closely fit the smooth curves generated by the model, and the values obtained for the merit function are sufficiently small: $F(m, \mu, P_0) = 13.1$ (Fig. 2a), $F(\lambda) = 0.16$ (Fig. 2b). This is a qualitative indicator of the goodness of fit of the model. When we quantitatively tested the goodness of fit for the SDD model (d.f. = 7) and LDD algorithm (d.f. = 5), we did not reject the null hypotheses that the data are derived from SDD model Eq. (1) and the LDD stochastic algorithm (SDD: $R^2 = 0.98$; LDD: $R^2 = 1$). The bootstrap estimates of the errors in an estimated parameter set are given in Table 1.

Table 1 shows that, overall, the model dynamics are sensitive to changes in infection efficiency, e, the initial density of the susceptible leaf area, S_0, the rate of spore production, ε, and the spore removal rate, μ. The impact of the variation of the contact rate, a, and the initial spore density, P_0, on the system dynamics was very low and negligible. Model Eq. (1) is relatively insensitive to the diffusion coefficient, δ, the LDD rate, λ, and the mortality rate of infectives, m.

3.3. Effect of crop heterogeneity on stratified pathogen spread

To compare the efficiency of the patterns (Table 2), we estimated the mean time for the disease severity to reach 80%, $T_{\mathrm{pt}}^{80\%}$ (d), and the relative spread deceleration, D_{pt} (%), pt∈ {pt1, pt′1, . . ., pt4, pt′4}, in each pattern, relative to the homogeneous susceptible field, pt0. A

Table 2
Planting patterns of susceptible (S) and resistant (R) varieties tested using the simulation model and the deceleration they produce of the spread of disease driven either by short-distance (SDD) or stratified dispersal (SDD + LDD). Susceptible host units are shown in black, and resistant host units in white. Mean deceleration values are given for each pattern, 95% CI values are shown in parenthesis. Deceleration is expressed as the percentage reduction of the disease spread observed compared to that in a simulated homogeneous susceptible crop pt0 (see text for the details).

Symbol	Pattern	S:R	Description	Deceleration (%)	
				SDD	SDD + LDD
pt1		1:1	Random mixture of susceptible and resistant varieties.	21	26.67 (26.66, 26.69)
pt′1		1:3		47	52.32 (52.3, 52.34)
pt2	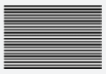	1:1	Narrow alternating rows of susceptible and resistant varieties.	18	21.06 (21.05, 21.08)
pt′2		1:3		36	23.28 (23.26, 23.3)
pt3		1:1	Wide alternating rows of susceptible and resistant varieties.	14	4.33 (4.32, 4.34)
pt′3		1:3		45	8.81 (8.79, 8.84)
pt4		1:1	Individual blocks of a susceptible variety scattered among resistant individuals.	19	28.36 (28.34, 28.38)
pt′4		1:3		28	62.33 (62.31, 62.36)

typical scenario of the stratified disease dispersal over pt0, generated by the full model with the estimated parameter set (Table 1) is illustrated in Fig. 3. The emergence of secondary foci accelerates epidemic spread up to $T_{pt0}^{80\%} = 62$ (d).

Table 2 summarizes the results of numerical simulations of the effects of spatial patterning of varietal mixtures on epidemic dynamics with short-distance and stratified dispersal. For an epidemic driven only by diffusive, short-distance dispersal (Table 2, SDD column), the pattern with the greatest slowing is a random 1:3 mixture (pt′1), which can lead to 47% spread deceleration compared to the purely homogeneous susceptible pattern (pt0). The random pattern (pt1) is the most effective for 1:1 mixtures, resulting in a 21% deceleration of spread. The effects of 1:1 remote blocks and frequent narrow rows (pt4, pt2) on pathogen spread are similar to that of the random pattern (pt1), 19% and 18% deceleration, respectively. Wide and distant rows of pt3 are the least effective of all 1:1 mixtures, leading to only 14% deceleration. However, in 1:3 mixtures the decelerating effect of wide rows (pt′3) is similar to the random pattern (pt′1), 45% and 47%, followed by narrow rows (pt′2), 36%. Remote blocks of a 1:3 mixture (pt′4) are the least effective 1:3 mixtures, producing only 28% deceleration.

For stratified invasion with long-distance dispersal (Table 2, SDD + LDD column), we found that the most efficient pattern is remote blocks (pt4, pt′4). In 1:1 mixture the deceleration effect of the remote blocks (pt4) could reach 28.36%, while in 1:3 mixtures (pt′4) they lead to 62.33%. Random patterns (pt1, pt′1) also significantly reduce the epidemic spread rate, about 26.67% for a 1:1 mixture, and 52.32% for a 1:3 mixture. Interestingly, 1:1 and 1:3 frequent narrow rows (pt3, pt′3) are almost equally effective, with 21.06–23.28% deceleration of spread. Wide and distant rows of patterns pt2 and pt′2 are ineffective in preventing the epidemic spread, as these patterns result in only 4.33% and 8.81% deceleration.

The comparison of SDD and stratified dispersal (Table 2, SDD and SDD + LDD columns) reveals that random mixtures (pt1, pt′1) are most effective against SDD, and fairly effective against an epidemic with a dual dispersal mechanism. Patterns with remote blocks (pt4, pt′4) are the best strategies for controlling stratified dispersal, but are much less effective against SDD. Frequent alternating rows (pt2, pt′2) have a moderate decelerating effect on both short- and long-distance dispersal. In the case of 1:3 mixtures, frequent alternating rows (pt′2) are a bit more effective in the context of short-distance dispersal than in that of disease spread by a dual dispersal mechanism. Wide, distant alternating rows (pt3, pt′3) are more effective against SDD than against stratified dispersal, especially when rarefied in space (pt′3).

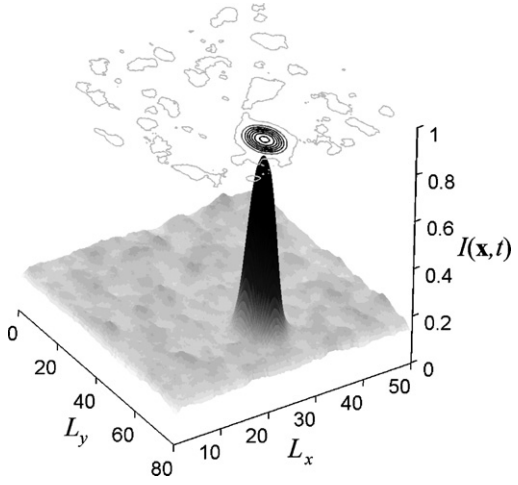

Fig. 3. Stratified dispersal of infectives $I(\mathbf{x}, t)$ over a homogenous susceptible field pt0. Contour lines depict secondary foci generated by long-distance spore dispersal from a source unit. Parameter values are presented in Table 1.

4. Discussion

We have examined the effects of spatial patterning of a varietal mixture on the airborne fungal disease dynamics driven by stratified dispersal. We built a spatially explicit model of the epidemic with a dual dispersal mechanism, involving both short- and long-distance dispersal, and parameterized it for the faba bean rust, to show that the pathogen's mode of dispersal considerably influences the efficacy of cultivar mixtures. Comparative analysis of the impact of cultivar mixtures on short-distance and stratified dispersal showed that the mixtures effective against stratified dispersal differed from those that are effective against short-distance dispersal. Our work demonstrates that the spatial arrangement of the mixture components in both agro-ecosystems and forestry has to accord with the modes of pathogen dispersal if the efficacy of crop diversification is to be maximized.

Our combined modelling approach presents a reasonably good fit to observed data on the spread of faba bean rust (Sache and Zadoks, 1996). The generality and simplicity of the proposed model means that it can be applied to the management of resource-mediated invasions by other airborne fungi, e.g., cereal rusts, apple scab, powdery mildew or potato late blight. The key problem is including spatial heterogeneity in a way that allows relatively

general conclusions to be drawn. This explains why so few epidemiological and invasion models include spatial structures. In this study we tried to solve this problem by a combined approach incorporating sufficient spatial realism and simplicity into the model to allow its parameterization for a real pathosystem. The model constructed for short-distance dispersal assumes that the pathogen population spreads like a wave travelling at constant velocity, which was once used as a paradigm in spatial plant disease epidemiology (Zadoks and Vandenbosch, 1994). Subsequent theoretical and experimental developments, however, have shown that the velocity of the wave consistently increases linearly with distance and exponentially with time (Shaw, 1995; Scherm, 1996; Cowger et al., 2005; Mundt et al., 2009). Coupling a diffusion model with a stochastic long-distance algorithm allows us to account for the impact of accelerating disease dispersal on the host–pathogen dynamics.

Carrying out simulations with realistic parameter values, we demonstrate that a smooth regular epidemic front caused by short-distance spore dispersal can be slowed by mixtures with markedly irregular structures, i.e., random patterns. Previous theoretical studies have shown that a threshold proportion of randomly protected sites can stop the fungal invasion of a susceptible population (Otten et al., 2004). Consistently with previous findings, randomization leading to highly irregular patterns is likely to be a key factor in determining the efficacy of cultivar mixtures against fungal disease spread by short-distance dispersal (Mundt et al., 1996). The effect of the spatial arrangement of susceptible and resistant varieties on the rate of spread of a disease is more pronounced in 1:3 mixtures. The increase in homogeneous surface in 1:3 mixtures results in the progressive loss of effectiveness. Our model shows that the transition from random patterning to remote homogeneous blocks can lead to a 40% loss of effectiveness. Alternating rows leads to 36% deceleration, whereas a random pattern results in 47% deceleration. Although random mixtures reportedly provide better disease control than alternating rows (Mundt and Leonard, 1985; Mundt, 2002; Didelot et al., 2007; Sapoukhina et al., 2009), row mixtures are easier to put into practice, and can be sufficiently effective for use in disease suppression at larger scales (Zhu et al., 2000). The efficiency of the row patterns can be improved if row width and the distance between rows are chosen rationally. Numerical simulations show that wide distant rows of a 1:3 mixture can be more effective than narrow rows in decelerating short-distance disease dispersal.

Our simulations predict that to combat stratified dispersal effectively, irregular patterns should be discontinuous and include a certain minimum distance between susceptible patches, decreasing the probability of infection by long-distance spore dispersal. This explains the good performance of patchy 1:3 mixtures, such as random and remote blocks, where the distance between susceptible patches is increased by the high proportion of resistant cultivars, which occupy 75% of the total surface. The failure of wide distant rows to control pathogen spread can be explained by the fact that the distance between the rows does not compensate for the continuity of the wide susceptible surface, which increases the probability of infection as a result of long-distance spore dispersal. We found that reducing the distance between susceptible patches in 1:1 mixtures reduced the effectiveness of the mixture in the context of stratified dispersal. Our results therefore show that in stratified dispersal, synergism between within-patch fragmentation and between-patch distance can improve the effectiveness of airborne plant disease management. This conclusion is consistent with the findings of multi-scale modelling of potato late blight epidemics. Skelsey (2008) demonstrated that to ensure effective suppression of late blight invasions, the fine-grain random distribution of potato fields should be coupled with within-field random varietal mixtures.

Combining a diffusion model for short-distance disease dispersal and a stochastic algorithm for long-distance dispersal allowed us to study the effects of spatial patterning of crop fields on disease dynamics driven by short-distance or stratified spore dispersal. We have shown that the spatial arrangement of the components of the varietal mixture has to accord with the mode of disease dispersal. Since our model is applicable to a broad range of spatial scales, it can be used to design suitable strategies for the geographical deployment of resistant cultivars and other sources of irregularity that could help to prevent the emergence and spread of disease. In the context of low input agriculture, it can be applied in to the management of pathogen invasion by intercropping and cultivar mixtures, and to the design of sustainable systems of land use. The reaction-diffusion model of continuous disease spread at constant speed could be used in the broader context of fungal invasions (Desprez-Loustau et al., 2007). We believe that the proposed modelling framework provides a way of applying theoretical investigations to solving practical problems in the management of airborne fungal disease in agro-ecosystems and forestry.

Acknowledgments

We would like to thank Christian Jost for helpful discussions about the implementation of the bootstrap method, and Valérie Caffier for assistance with parameter estimation. Funding for this research was provided by the French Ministry of Agriculture (grant CTPS-B044500). The first author's postdoc was funded by the U.S. Civilian Research and Development Foundation for the Independent States of the Former Soviet Union (CRDF), INAPG (now AgroParisTech), the Région Île-de-France and INRA.

References

Andow, D.A., Kareiva, P.M., Levin, S.A., Okubo, A., 1990. Spread of invading organisms. Landscape Ecol. 4, 177–188.

Aubertot, J.N., Barbier, J.M., Carpentier, A., Gril, J.J., Guichard, L., Lucas, P., Savary, S., Savini, I., Voltz, M. (Eds.), 2005. Pesticides, agriculture et environnement. Réduire l'utilisation des pesticides et en limiter les impacts environnementaux. Expertise report. INRA, Paris, 64 pp.

Bayles, R.A., Flath, K., Hovmøller, M.S., de Vallavieille-Pope, C., 2000. Breakdown of the *Yrl7* resistance to yellow rust of wheat in northern Europe. Agronomie 20, 805–811.

Bouws, H., Finckh, M.R., 2008. Effects of strip intercropping of potatoes with non-hosts on late blight severity and tuber yield in organic production. Plant Pathol. 57, 916–927.

Cowger, C., Wallace, L.R.D., Mundt, C.C., 2005. Velocity of spread of wheat stripe rust epidemics. Phytopathology 95, 972–982.

Desprez-Loustau, M.L., Robin, C., Buée, M., Courtecuisse, R., Garbaye, J., Suffert, F., Sache, I., Rizzo, D.M., 2007. The fungal dimension of biological invasions. Trends Ecol. Evol. 22, 472–480.

Didelot, F., Brun, L., Parisi, L., 2007. Effects of cultivar mixtures on scab control in apple orchards. Plant Pathol. 56, 1014–1022.

Efron, B., Tibshirani, R.J., 1993. An Introduction to the Bootstrap. Chapman and Hall, London, 456 pp.

Finckh, M.R., Wolfe, M.S., 2006. Diversification strategies. In: Cooke, B.M., Jones, D.G., Kaye, B. (Eds.), The Epidemiology of Plant Diseases. Springer, Dordrecht, pp. 269–307.

Guérin, F., Le Cam, B., 2004. Breakdown of the scab resistance gene Vf in apple leads to a founder effect in populations of the fungal pathogen *Venturia inaequalis*. Phytopathology 94, 364–369.

Hengeveld, B., 1989. Dynamics of Biological Invasions. Chapman and Hall, London, 160 pp.

Hengeveld, B., 1994. Small-step invasion research. Trends Ecol. Evol. 9, 339–342.

Higgins, S.I., Richardson, D.M., 1999. Predicting plant migration rates in a changing world: the role of long-distance dispersal. Am. Nat. 153, 464–475.

Jin, Y., Szabo, L.J., Pretorius, Z.A., Singh, R.P., Ward, R.W., Fetch Jr., T., 2008. Detection of virulence to resistance gene *Sr24* within race TTKS of *Puccinia graminis* f. sp. *tritici*. Plant Dis. 92, 923–926.

Manthey, R., Fehrmann, H., 1993. Effect of cultivar mixtures in wheat on fungal diseases, yield and profitability. Crop Prot. 12, 63–68.

Mundt, C.C., 2002. Use of multiline cultivars and cultivar mixtures for disease management. Annu. Rev. Phytopathol. 40, 381–410.

Mundt, C.C., Leonard, K.J., 1985. Effect of host genotype unit area on epidemic development of crown rust following focal and general inoculations of mixtures of immune and susceptible oat plants. Phytopathology 75, 1141–1145.

Mundt, C.C., Brophy, L.S., Kolar, S.C., 1996. Effect of genotype unit number and spatial arrangement on severity of yellow rust in wheat cultivar mixtures. Plant Pathol. 45, 215–222.
Mundt, C.C., Sackett, K.E., Wallace, L.D., Cowger, C., Dudley, J.P., 2009. Long-distance dispersal and accelerating waves of disease: empirical relationships. Am. Nat. 173, 456–466.
Murray, J.D., 1993. Mathematical Biology. Springer-Verlag, New York, 767 pp.
Nathan, R., Perry, G., Cronin, J.T., Strand, A.E., Cain, M.L., 2003. Methods for estimating long-distance dispersal. Oikos 103, 261–273.
Okubo, A., Levin, S.A. (Eds.), 2002. Diffusion and Ecological Problems: Modern Perspectives, 2nd ed. Springer-Verlag, New York, 467 pp.
Otten, W., Bailey, D.J., Gilligan, C.A., 2004. Empirical evidence of spatial thresholds to control invasion of fungal parasites and saprotrophs. New Phytol. 163, 125–132.
Press, W.H., Teukolsky, S.A., Vetterling, W.T., Flannery, B.P., 1992. Numerical Recipes in C: The Art of Scientific Computing, 2nd ed. Cambridge University Press, London, 1235 pp.
Rouxel, T., Penaud, A., Pinochet, X., Brun, H., Gout, L., Delourme, R., Schmit, J., Balesdent, M.H., 2003. A 10-year survey of populations of *Leptosphaeria maculans* in France indicates a rapid adaptation towards the Rlm1 resistance gene of oilseed rape. Eur. J. Plant Pathol. 109, 871–881.
Sache, I., Zadoks, J.C., 1995. Life table analysis of faba bean rust. Eur. J. Plant Pathol. 101, 431–439.
Sache, I., Zadoks, J.C., 1996. Spread of faba bean rust over a discontinuous field. Eur. J. Plant Pathol. 102, 51–60.
Sapoukhina, N., Durel, Ch.-E., Le Cam, B., 2009. Spatial deployment of gene-for-gene resistance governs evolution and spread of pathogen populations. Theor. Ecol. 2, 229–238.
Scherm, H., 1996. On the velocity of epidemic waves in model plant disease epidemics. Ecol. Model. 87, 217–222.
Shaner, G., Finney, R.E., 1977. The effect of nitrogen fertilization on the expression of slow-mildewing resistance in Knox wheat. Phytopathology 67, 1051–1056.
Sharov, A.A., Liebhold, A.M., 1998. Model of slowing the spread of gypsy moth (Lepidoptera: Lymantriidae) with a barrier zone. Ecol. Appl. 8, 1170–1179.
Shaw, M.W., 1995. Simulation of population expansion and spatial pattern when individual dispersal distributions do not decline exponentially with distance. P. Roy. Soc. Lond. B Biol. 259, 243–248.
Shigesada, N., Kawasaki, K., 1997. Biological Invasions: Theory and Practice. Oxford University Press, Oxford, 205 pp.
Shigesada, N., Kawasaki, K., Takeda, Y., 1995. Modeling stratified diffusion in biological invasions. Am. Nat. 146, 229–251.
Singh, R.P., Hodson, D.P., Jin, Y., Huerta-Espino, J., Kinyua, M.G., Wanyera, R., Njau, P., Ward, R.W., 2006. CAB Rev.: Persp. Agric. Vet. Sci. Nutr. Nat. Res. 054, 1–13.
Skellam, J.G., 1951. Random dispersal in theoretical populations. Biometrika 38, 196–218.
Skelsey, P., 2008. Multi-scale modeling of potato late blight epidemics. PhD thesis. Wageningen University, 272 pp.
Skelsey, P., Rossing, W.A.H., Kessel, G.J.T., Powell, J., van der Werf, W., 2005. Influence of host diversity on development of epidemics: an evaluation and elaboration of mixture theory. Phytopathology 95, 328–338.
Soubeyrand, S., Enjalbert, J., Sanchez, A., Sache, I., 2007. Anisotropy, in density and in distance, of the dispersal of yellow rust of wheat: experiments in large field plots and estimation. Phytopathology 97, 1315–1324.
Van Den Bosch, F., Gilligan, C.A., 2003. Longevity and deployment of resistance. Phytopathology 93, 616–625.
Xu, X.M., Ridout, M.S., 2000. Stochastic simulation of the spread of race-specific and race-nonspecific aerial fungal pathogens in cultivar mixtures. Plant Pathol. 49, 207–218.
Zadoks, J.C., Vandenbosch, F., 1994. On the spread of plant disease: a theory on foci. Annu. Rev. Phytopathol. 32, 503–521.
Zhu, Y.Y., Chen, H.R., Fan, J.H., Wang, Y.Y., Li, Y., Chen, J.B., Fan, J.X., Yang, S.S., Hu, L.P., Leung, H., Mew, T.W., Teng, P.S., Wang, Z., Mundt, C.C., 2000. Genetic diversity and disease control in rice. Nature 406, 718–722.